Chemical Physics Letters 507 (2011) 229–233

Contents lists available at ScienceDirect

Chemical Physics Letters

journal homepage: www.elsevier.com/locate/cplett

Structural studies of the water pentamer

Frank Ramírez [a], C.Z. Hadad [a], Doris Guerra [a], Jorge David [b], Albeiro Restrepo [a,*]

[a] Instituto de Química, Universidad de Antioquia, AA 1226 Medellín, Colombia
[b] Escuela de Ciencias y Humanidades, Departamento de Ciencias Básicas, Universidad Eafit, AA 3300, Medellín, Colombia

ARTICLE INFO

Article history:
Received 25 October 2010
In final form 23 March 2011
Available online 30 March 2011

ABSTRACT

A computational study of the water pentamer gas phase conformational space is reported in this Letter. Forty-four stationary points distributed among 12 structural patterns were located at the MP2/6–311++G(d,p) level. At least 5 geometrical motifs (25 structures) are predicted within 3 kcal/mol of the most stable conformation at the CCSD(T)/aug–cc–pVTZ//MP2/6–311++G(d,p) level. We show evidence that dipole–dipole interactions are at play in stabilizing the clusters. Electron densities and their Laplacians at the hydrogen bond critical points were found to be linearly correlated with relative energies for all clusters. Logarithmic relationships were found for the $[\mathbf{r}_{eq}, \rho(\mathbf{r}_c)]$ and $[\mathbf{r}_{eq}, \nabla^2\rho(\mathbf{r}_c)]$ pairs in all hydrogen bonds.

1. Introduction

Vasts amounts of scientific literature are devoted to water and to hydrogen bonding, two connected problems with many unresolved issues. The structure of liquid water is not known, however, bulk liquid water is often described as a collection of hydrogen-bonded clusters instead of an isotropic medium [1]. The comparative weakness of hydrogen bonds relative to chemical bonds allows their easy formation and breaking at ambient conditions [2], leading to rich conformational spaces for systems stabilized via hydrogen-bonding networks (HBNs), thus increasing the contributions from many clusters varying in both structure and size to the liquid and gas phases of such systems. Characterization of these already complex conformational spaces is complicated by intricate dynamics for HBNs rearrangements [3–6]. Since many of the unusual properties of water are thought to arise from behavior, interaction, and interconversion of the constituting clusters, a detailed knowledge of the possibilities of cluster formation and of their geometries and properties is needed for proper descriptions of water.

Except for the pioneer work in the several experimental reports by Saykally and collaborators, and for a number of theoretical endeavours by other authors, it appears as if the water pentamer (W_5 hereforth) has not been as extensively studied as other water microclusters. Xantheas and Dunning predicted via ab initio calculations a puckered pentagonal ring as the global minimum for W_5 [7]. The existence of W_5 clusters in supersonic expansions was later confirmed in infrared cavity ringdown laser absorption spectroscopy (IR-CRLAS) experiments [8]. It has been shown by means of Terahertz VRT spectroscopy [3,4] that pentamer puckered rings vibrationally average to a symmetric, heavy-atom-quasi-planar structure. Shields and coworkers have suggested that cyclic tetramers and pentamers would be the most significant cyclic water clusters in the atmosphere [9–11].

Theoretical calculations mainly use the cyclic pentamer to evaluate the efficiency of theoretical methods, or to investigate evolution of properties of water clusters of increasing sizes [9,12–17]. A methodic characterization of the W_5 PES was given by Miyake and Aida [18], they reported 161 topologically different hydrogen bonding patterns that produced a few geometrical motifs and a total of 21 stable minima at the HF/6–31G* level. Another exhaustive exploration of the W_5 PES was given by Day and coworkers [11]; their search led to 10 stable minima spread into 4 geometrical motifs, from an initial set of 20736 initial candidates which where subjected to successive PM3, HF/6–31G* and G3 treatments.

In this work, we present a stochastic exploration of the W_5 PES to produce candidate structures for local minima, which are further optimized and characterized by means of second order perturbation theory calculations at the MP2/6–311++G(d,p) level, followed by highly correlated CCSD(T)/aug–cc–pVTZ single point energy calculations. Our goal is to contribute to the still limited understanding of this very important PES.

2. Computer methods

We used the molecular cluster capabilities of the ASCEC program [19] which contains a modified Metropolis acceptance test in an adapted version of the Simulated Annealing optimization procedure. The annealing algorithm [20–22] was used to generate candidate structures after random walks of the PM3 PES. The hybrid B3LYP density functional in conjunction with the 6–311++G(d,p) basis set was used to optimize and characterize the structures afforded by ASCEC. Further refinement and characterization of the stationary

* Corresponding author.
E-mail address: albeiro@matematicas.udea.edu.co (A. Restrepo).

0009-2614/$ - see front matter © 2011 Elsevier B.V. All rights reserved.
doi:10.1016/j.cplett.2011.03.084

points was carried out by using second order perturbation theory at the MP2/6–311++G(d,p) level. Analytical harmonic second derivative calculations were used to characterize all stationary points as true minima (no negative eigenvalues of the Hessian matrix). Highly correlated CCSD(T) energies were calculated on all the MP2 located minima using the aug–cc–pVTZ basis set. This methodology has been previously used in the study of small hydrogen bonded networks, specifically the water tetramer [23], the water hexamer [24], the methanol tetramer [25], and the carbonic acid dimer [26].

Binding energies (BE) were calculated by subtracting the energy of the given pentamer from five times the energy of the water monomer, in this way, larger positive numbers correspond to larger stabilization energies. Relative binding energies ΔBE were calculated as the difference between the energy of the most stable pentamer and the energy of a particular structure. We used the MP2/6–311++G(d,p) ZPEs to correct the CCSD(T) electronic energies in the calculations of binding energies and relative stabilities. There are several reports that clearly reveal the failure of counterpoise correction for basis set superposition error in the study of small hydrogen-bonded clusters; specific cases are the dimers of carbonic acid $(H_2CO_3)_2$ [26,27], hydrofluoric acid HF_2 [28,29], and water $(H_2O)_2$ [30]. Theoretical treatment of the methanol tetramer [25], showed no significant differences by correcting for BSSE. Therefore, in this work, we restrain ourselves from applying such methodology. All optimization, frequency, and energy calculations were carried out using the Gaussian 03 suite of programs [31]. Isomer populations were estimated by standard Boltzmann distribution analysis. Topological analysis of the electron densities were carried out along the lines implemented in the DGrid 4.5 program [32].

3. Results and discussion

3.1. ASCEC conditions

We used two variations of the big bang approach to construct the initial geometries for all ASCEC runs: one strategy was to place the five water molecules at the same position allowing them to evolve under the annealing conditions; a second alternative was to superimpose one water molecule with each of the eight tetramers reported in the literature [23] and running the annealing on the resulting systems. Whatever the choice, the systems were placed inside cubes of 7 and 8 Å of length; the PM3 semiempirical Hamiltonian was used to calculate the energy of a Markovian chain of randomly generated pentamer configurations; we used geometrical quenching routes with initial temperature of 400 K, a constant temperature decrease of 5% and 100 total temperatures.

3.2. Geometries and structural issues

The W_5 equilibrium geometries were produced following the procedure outlined above. All geometry optimizations were carried out with no imposition of symmetry constraints as the structures coming from ASCEC are randomly generated and belong to the C_1 point group, however some of the located stationary points have higher effective (heavy-atom) symmetries.

We found 44 distinct molecular clusters distributed among 12 different geometrical motifs on the MP2/6–311++G(d,p) PES; the structural motifs along with a subjective descriptive notation are shown in approximate decreasing order of stability according to the CCSD(T)//MP2 calculations in Figure 1. An interesting observation is that despite the W_5 structures having no chiral centers, we found several enantiomer pairs due to the overall spatial arrangements of the clusters.

There are plenty of possibilities for each geometrical motif and surely many more structures to be found: recall the 21 stable minima distributed among a few geometrical motifs found by Miyake and Aida at the HF/6–31G* level [18]; in the related case of the water hexamer, 14 and 27 isomers were reported just for the W_6 cage alone in two independent reports [33,34]. The rich PES obtained in this study is a consequence of the stochastic nature of the search of the quantum conformational space performed by the ASCEC program, which bypasses the structure-guessing step in the search for local minima [23,35]. Similar structural complexities have been observed in the study of other hydrogen-bonded microclusters [23–26].

3.3. Energies, cluster stabilization and other properties

A number of important observations are drawn from Table 1, which summarizes the relevant energy related quantities:

(i) There are at least five distinct geometrical motifs (25 structures) within 3 kcal/mol of the most stable structure. Since there are several conformational possibilities for the hydrogen atoms not taking part in the stabilizing hydrogen bonding network, it follows that the low energy states for W_5 are densely populated by a multitude of structures.

(ii) The most stable structure is a heavy-atom slightly puckered, quasi-planar ring. The most stable structures for W_4 and W_6 are heavy-atom planar and 3-dimensional, respectively [23,24], this indicates that for $n \geqslant 6$, 3D conformations are preferred in water microclusters. An explanation for such structural preferences has been proposed [36], it involves the realization that cage critical points are present in water microclusters only for $n \geqslant 6$.

(iii) Structures with side chains and dangling molecules are the least stable ones. The apparent high stability of the Tetramer + 1 isomer is provided by the contribution from the very stable tetramer conformation.

Electrostatic interactions have been suggested as significant stabilization factors for hydrogen bonded microclusters [13,23–26,37–39]. For the water tetramer [23], hexamer [24], the methanol tetramer [25], and the carbonic acid dimer [26], the electrostatic contributions to cluster stabilization have been postulated to arise from orientations of the dipole components along polar bonds, resulting in networks of favorable dipole–dipole interactions. The same type of networks are encountered here for the W_5 clusters. We calculated the total electrostatic energy from contributions of all Mulliken predicted atom charges belonging to the stabilizing hydrogen bonding network. Dipole–dipole interaction energies are calculated within the multipole expansion by $[\mathbf{p}_1 \cdot \mathbf{p}_2 - 3(\mathbf{n} \cdot \mathbf{p}_1)(\mathbf{n} \cdot \mathbf{p}_2)]/4\pi\epsilon_0|\mathbf{x}_1 - \mathbf{x}_2|^3$; where $\mathbf{p}_i$ are the dipole vectors located at $\mathbf{x}_i$ and $\mathbf{n}$ a unit vector in the $(\mathbf{x}_1 - \mathbf{x}_2)$ direction [40]. The multipole expansion requires conditions not met in our case, namely ideal dipoles and that the distances between individual dipoles must be very large compared to the distance separating the charges of individual dipoles; therefore, as an indirect measure of the dipole–dipole interactions, we calculated the total electrostatic energy for the interactions of all point charges at the positions of the atoms belonging to dipole components along the hydrogen bonding network. Figure 2 shows relative stabilization energies calculated for all clusters at all levels of theory reported in this work in addition to the total electrostatic energy for the interactions of all point charges at the positions of the atoms belonging to dipole components along the hydrogen bonds for all the structures. A good trend agreement between the curves is observed, giving strong support to the dipole–dipole stabilization hypothesis for the W_5 clusters.

From Figure 1 and Table 1, we point out that for the same number of water molecules, cluster stability is not directly related to the

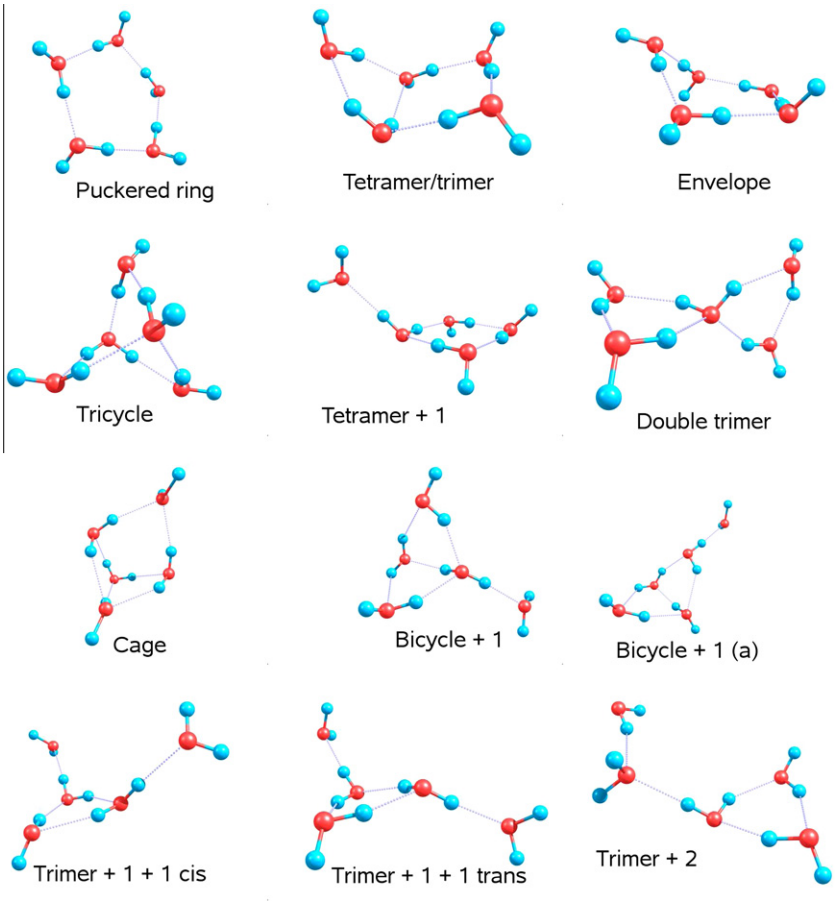

Figure 1. Gas phase MP2/6–311++G(d,p) structures of the geometrical motifs for the water pentamers.

Table 1
Energetic analysis for the $(H_2O)_5$ clusters. ΔE: relative energy with respect to the most stable structure at each level. BE: binding energy. All CCSD(T)/aug–cc–pVTZ calculations using the MP2/6–311++G(d,p) optimized geometries. All relative and binding energies corrected for the unscaled MP2/6–311++G(d,p) ZPEs. All energies in kcal/mol. Isomer contributions $\%x_i$ estimated via standard Boltzmann population analysis.

Structure	BE CCSD(T)	BE MP2	ΔE CCSD(T)	ΔE MP2	ΔGibbs[a] MP2	$\%x_i$ CCSD(T)	$\%x_i$ MP2	$\%x_i$ Gibbs[a]
Puckered ring	25.9	30.2	0.0	0.0	0.0	63	81	73
Tetramer/trimer	25.1	28.7	0.8	1.5	2.0	15	6	2
Envelope	24.9	29.1	1.0	1.2	0.7	12	11	23
Tricycle	24.7	27.7	1.2	2.5	3.5	9	1	0.2
Tetramer + 1	22.9	26.6	3.0	3.6	2.5	0.4	0.2	1
Double trimer	21.7	24.6	4.2	5.7	5.5	≈ 0	≈ 0	≈ 0
Cage	20.0	22.0	5.9	8.2	8.6	≈ 0	≈ 0	≈ 0
Bicycle + 1	19.7	22.0	6.2	8.2	6.8	≈ 0	≈ 0	≈ 0
Bicycle + 1 (a)	19.2	21.5	6.7	8.8	6.8	≈ 0	≈ 0	≈ 0
Trimer + 1 + 1 *cis*	16.9	19.8	9.0	10.4	7.1	≈ 0	≈ 0	≈ 0
Trimer + 1 + 1 *trans*	16.8	19.8	9.1	10.4	7.0	≈ 0	≈ 0	≈ 0
Trimer + 2	16.5	19.0	9.4	11.2	6.9	≈ 0	≈ 0	≈ 0

[a] Calculated as G = H–TS, $T = 298.16$ K.

number of hydrogen bonds nor to the number of rings: puckered ring and trimer +2, the most and least stable structures, respectively, have exactly the same number of hydrogen bonds (5) and rings (1), while cage, the 7th structure in the stability order, ≈6 kcal/mol above puckered ring, has 8 hydrogen bonds and 4 rings.

3.4. Topological analysis of the electron densities

There is a long and successful history of using Bader's quantum theory of atoms in molecules (QTAIM) to study hydrogen bonded systems. In this work, we are interested in properties evaluated at hydrogen bond critical points (HBCPs). In particular, $\rho(\mathbf{r}_c), \nabla^2\rho(\mathbf{r}_c)$, the electron densities at the bond critical points and their Laplacians have been shown to contain very useful information about hydrogen bonds and their properties. Closed shell interactions, hydrogen bonds among them, are characterized by positive values of $\nabla^2\rho(\mathbf{r}_c)$ and low (<0.1) values for $\rho(\mathbf{r}_c)$ [41].

Knop and coworkers found an inverse power correlation between several types of calculated S–S bonds with the electron densities at the bond critical points [42]. Similar relationships were previously shown to exist for other types of bonds, which led the authors to suggest that $[\mathbf{r}_{eq}, \rho(\mathbf{r}_c)]$ relationships (bond length, elec-

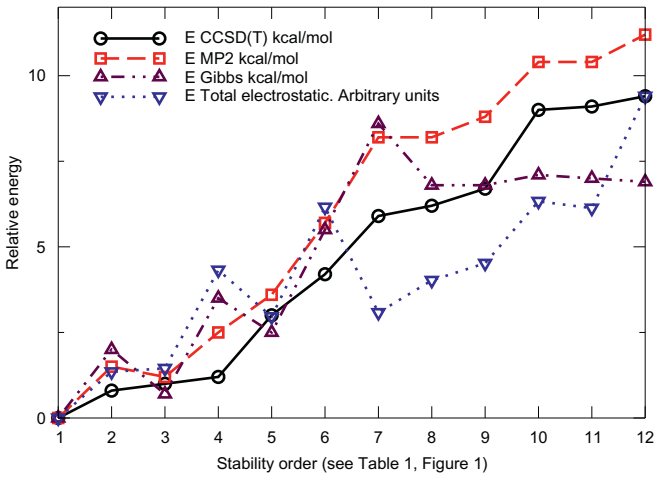

Figure 2. Stabilization energies at several levels of theory for the W_5 clusters.

tron density at the bond critical point) exist for any class of binary bonds, regardless of the origin and magnitude of the individual contributions from particular molecular orbitals to the electron densities at the BCPs. A later study by Alkorta et al. [43], considering many types of bonds, seems to validate this hypothesis, reporting logarithmic $[\mathbf{r}_{eq}, \rho(\mathbf{r}_c)]$ correlations with larger slopes for hydrogen bonds than for covalent bonds; fitting the data to logarithmic functions leads to the expected decay in electron density at the BCPs as the bond lengths grow to increasingly larger values. Further support for the above hypothesis was provided by studying large sets of systems exhibiting N–H···N hydrogen bonds [44,45]; the results of these studies also show, among many other pairs, strong $[\mathbf{r}_{eq}, \rho(\mathbf{r}_c)]$ and $[\mathbf{r}_{eq}, \nabla^2\rho(\mathbf{r}_c)]$ correlations, and that covalent and hydrogen bonds are better described by separate fittings.

Linear relationships were found earlier for the $[E_{HB}, \rho(\mathbf{r}_c)]$, and for the $[E_{HB}, \nabla^2\rho(\mathbf{r}_c)]$ pairs (E_{HB} being the energy of the hydrogen bonds) for series of nitriles interacting via hydrogen bonds with HF and HCl [46,47].

Topological analysis of the electron densities for W_5 in this study suggest linear relationships between the sum of the electron densities at all HBCPs for a given cluster and its relative stability ($[\sum \rho(\mathbf{r}_c), \Delta E]$ pair); a similar linear trend is predicted for the sum

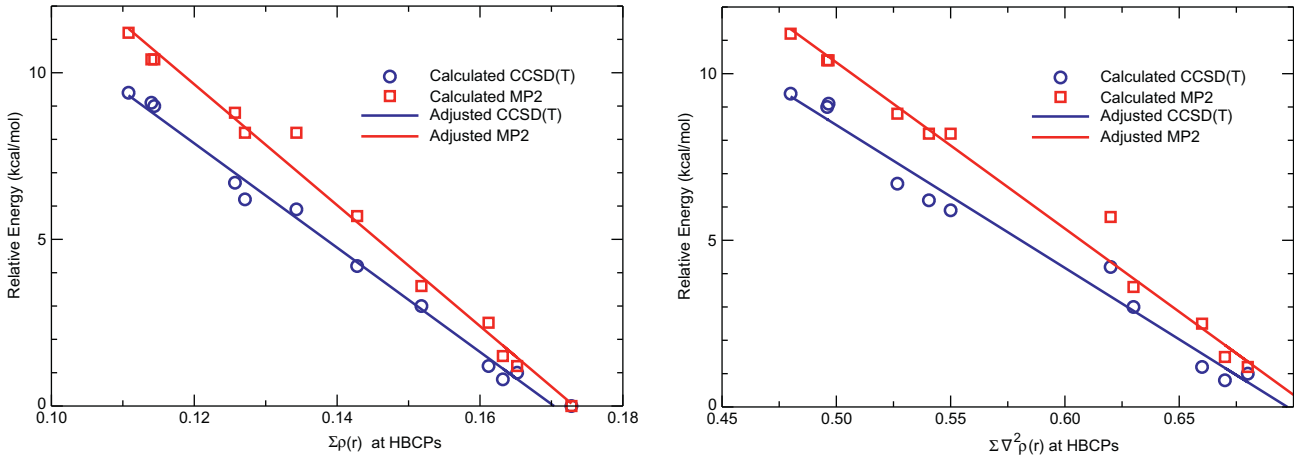

Figure 3. Relationship between the sum of densities at the hydrogen bond critical points (left) and the sum of the Laplacians of the densities at the HBCPs (right) with the relative energies for the W_5 clusters. Energies calculated at the CCSD(T)/aug–cc–pVTZ//MP2/6–311++G(d,p) and MP2/6–311++G(d,p) levels. All calculations using the MP2/6–311++G(d,p) densities.

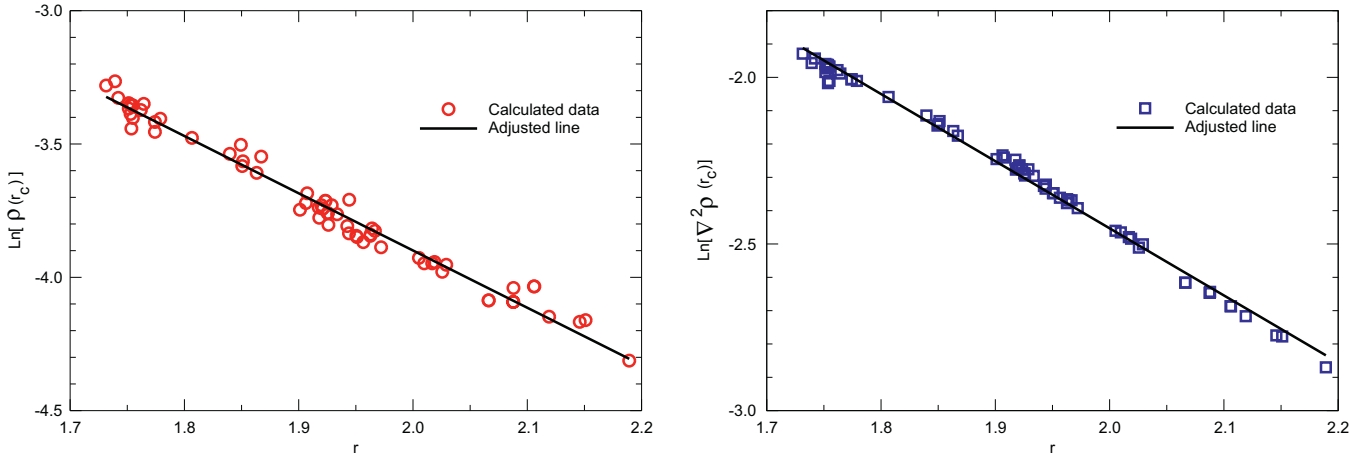

Figure 4. Logarithmic relationships for the $[\mathbf{r}, \rho(\mathbf{r}_c)]$ (left) and $[\mathbf{r}, \nabla^2\rho(\mathbf{r}_c))]$ (right) pairs. **r** being the length of the hydrogen bonds. Densities and Laplacians of the densities in atomic units. Bond lengths in Å. Adjusted equations: $\ln[\rho(\mathbf{r}_c)] = 0.394 - 2.147\mathbf{r}$, $R^2 = 0.98$ and $\ln\left[\nabla^2\rho(\mathbf{r}_c)\right] = 1.576 - 2.015\mathbf{r}$, $R^2 = 0.99$.

of the Laplacians of the densities at the same HBCPs ($[\sum \nabla^2\rho(\mathbf{r}_c), \Delta E]$ pair), see Figure 3. These results are in excellent agreement with previous indications that $\rho(\mathbf{r}_c)$ and $\nabla^2\rho(\mathbf{r}_c)$ can be used to characterize the strength of hydrogen bonds [48]: here, higher concentrations of electron densities in the interaction regions lead to stronger hydrogen bonds, similarly, higher values for the Laplacians of the electron densities, that is, more ionic and less covalent character of the hydrogen bonds also lead to more stable structures; this observation strongly supports the above discussed dipole–dipole stabilization hypothesis for the W_5 clusters. Figure 4 shows very good logarithmic correlations for the $[\mathbf{r}_{eq}, \rho(\mathbf{r}_c)], [\mathbf{r}_{eq}, \nabla^2\rho(\mathbf{r}_c)]$ pairs, in agreement with the several previously reported trends discussed above [42–47].

4. Concluding remarks

We report the geometries and properties of 12 structural patterns located on the MP2/6–311++G(d,p) PES of the water pentamer. Forty-four distinct clusters were obtained in all. The structures were found after random walks of the PM3 PES. A Boltzmann distribution analysis reveals several isomers with significant populations. There are at least 5 structural patterns (25 structures) within 3 kcal/mol of the most stable conformation. There are well established linear correlations between the relative stabilities of the clusters and the sums of the densities ($[\sum \rho(\mathbf{r}_c), \Delta E]$ pair) and between the relative stabilities and the sums of the Laplacians of the densities at all HBCPs ($[\sum \nabla^2\rho(\mathbf{r}_c), \Delta E]$ pairs). Very good logarithmic relationships were also found for the $[\mathbf{r}_{eq}, \rho(\mathbf{r}_c)], [\mathbf{r}_{eq}, \nabla^2\rho(\mathbf{r}_c)]$ pairs. Electrostatic forces in the form of dipole–dipole interactions are major contributors to the stabilization of the molecular clusters. MP2/6–311++G(d,p) and CCSD(T)/aug–cc–pVTZ//MP2/6–311++G(d,p) model chemistries are in good agreement for binding energy calculations.

Acknowledgements

Partial funding for this work by Universidad EAFIT, internal project number 261-00002 is acknowledged. Financial support from Universidad de Antioquia, CODI office is also acknowledged. Professor Samantha Jenkins, Hunan Normal University, Hunan, China, gave us very useful insights about this problem, her help is greatly appreciated.

References

[1] R. Ludwig, Angew. Chem. Intl. Ed. 40 (2001) 1808.
[2] A. Buckingham, J. Bene, S. McDowell, Chem. Phys. Lett. 463 (2009) 1.
[3] H. Harker, M. Viant, M. Keutsch, E. Michael, R. McLaughlin, R. Saykally, J. Phys. Chem. A 109 (2005) 6483.
[4] M. Brown, M. Keutsch, R. Saykally, J. Chem. Phys. 109 (1998) 9645.
[5] M. Keutsch, R. Saykally, PNAS 98 (2001) 10533.
[6] M. Viant, J. Cruzan, D. Lucas, M. Brown, K. Liu, R. Saykally, J. Phys. Chem. A 101 (1997) 9032.
[7] S. Xantheas, T. Dunning, J. Chem. Phys. 99 (1993) 8774.
[8] J. Paul, C. Collier, R. Saykally, J. Scherer, A. Okeefe, J. Phys. Chem. A 101 (1997) 5211.
[9] M. Dunn, E. Pokon, G. Shields, Int. J. Quantum Chem. 100 (2004) 1065.
[10] M. Dunn, E. Pokon, G. Shields, J. Am. Chem. Soc. 126 (2004) 2647.
[11] M. Day, K. Kirschner, G. Shields, J. Phys. Chem. A 109 (2005) 6773.
[12] S. Xantheas, C. Burnham, R. Harrison, J. Chem. Phys. 116 (2002) 1493.
[13] A. Sediki, F. Lebsir, L. Martiny, M. Dauchez, A. Krallafa, Food Chem. 106 (2008) 1476.
[14] S. Maheshwary, N. Patel, S. Sathyamurthy, A. Kulkarni, S. Gadre, J. Phys. Chem. A 105 (2001) 10525.
[15] M. Hodges, J. Stone, S. Xantheas, J. Phys. Chem. A 101 (1997) 9163.
[16] S. Xantheas, Chem. Phys. 258 (2000) 225.
[17] B. Hartke, M. Schütz, H. Werner, Chem. Phys. 239 (1998) 561.
[18] T. Miyake, M. Aida, Internet Eletron. J. Mol. Des. 2 (2003) 24.
[19] J. Pérez, A. Restrepo, ASCEC V-02: Annealing Simulado con Energía Cuántica. Property, Development and Implementation: Grupo de Química–Física Teórica, Instituto de Química, Universidad de Antioquia: Medellín, Colombia, 2008.
[20] N. Metropolis, A. Rosenbluth, M. Rosenbluth, A. Teller, E. Teller, J. Chem. Phys. 21 (1953) 1087.
[21] S. Kirkpatrick, C. Gellat, M. Vecchi, Science 220 (1983) 671.
[22] E. Aarts, H. Laarhoven, Simulated Annealing, Springer, New York, 1987.
[23] J. Pérez, C. Hadad, A. Restrepo, Int. J. Quantum Chem. 108 (2008) 1653.
[24] G. Hincapié, N. Acelas, M. Castaño, J. David, A. Restrepo, J. Phys. Chem. A 114 (2010) 7809.
[25] J. David, D. Guerra, A. Restrepo, J. Phys. Chem. A 113 (2009) 10167.
[26] J. Murillo, J. David, A. Restrepo, Phys. Chem. Chem. Phys. 12 (2010) 10963.
[27] K. Liedl, S. Sekušak, E. Mayer, J. Am. Chem. Soc. 119 (1997) 3782.
[28] K. Peterson, T. Dunning, J. Chem. Phys. 102 (1995) 2032.
[29] S. Xantheas, J. Chem. Phys. 104 (1996) 8821.
[30] M. Feyereisen, D. Dixon, J. Phys. Chem. 100 (1996) 2993.
[31] M.J. Frisch et al., Gaussian 03, Revision E.01, Gaussian, Inc., Wallingford CT, 2004.
[32] M. Kohout, DGrid, version 4.5, Radebeul, 2009.
[33] J. Gregory, D. Clary, J. Phys. Chem. A 101 (1997) 6813.
[34] M. Tissandier, S. Singer, J. Coe, J. Phys. Chem. A 104 (2000) 752.
[35] J. Pérez, E. Flórez, C. Hadad, P. Fuentealba, A. Restrepo, J. Phys. Chem. A 112 (2008) 5749.
[36] S. Jenkins, A. Restrepo, J. David, D. Yin, S. Kirk, Phys. Chem. Chem. Phys., submitted for publication.
[37] L. Ojamäe, K. Hermansson, J. Phys. Chem. 98 (1994) 4271.
[38] B. King, F. Weinhold, J. Chem. Phys. 103 (1995) 333.
[39] M. Masella, J. Flament, J. Chem. Phys. 108 (1999) 7141.
[40] J. Jackson, Classical Electrodynamics, 3rd ed., Wiley, New York, 1998.
[41] R. Bader, H. Essen, J. Chem. Phys. 80 (1984) 1943.
[42] O. Knop, R. Boyd, S. Choi, J. Am. Chem. Soc. 110 (1988) 7299.
[43] I. Alkorta, I. Rozas, J. Elguero, Struct. Chem. 9 (1998) 243.
[44] O. Knop, K. Rankin, R. Boyd, J. Phys. Chem. A 105 (2001) 6552.
[45] O. Knop, K. Rankin, R. Boyd, J. Phys. Chem. A 107 (2003) 272.
[46] R. Boyd, S. Choi, Chem. Phys. Lett. 120 (1985) 80.
[47] R. Boyd, S. Choi, Chem. Phys. Lett. 129 (1986) 62.
[48] R. Gillespie, P. Popelier, Chemical Bonding and Molecular Geometry, Oxford, New York, 2001.